

# The Crystal Structure of a Parallel-stranded Guanine Tetraplex at 0.95 Å Resolution

Kathryn Phillips<sup>1</sup>, Zbyszek Dauter<sup>2</sup>, Alastair I. H. Murchie<sup>3</sup>  
David M. J. Lilley<sup>3</sup> and Ben Luisi<sup>1\*</sup>

<sup>1</sup>Department of Biochemistry  
Cambridge University  
Tennis Court Road, Cambridge  
CB2 1QW, UK

<sup>2</sup>Department of Chemistry  
York University, Heslington  
York YO1 5DD, UK

<sup>3</sup>CRC Nucleic Acid Structure  
Research Group, Department of  
Biochemistry, Dundee  
University, Dundee DD1 4HN  
UK

In both DNA and RNA, stretches of guanine bases can form stable four-stranded helices in the presence of sodium or potassium ions. Sequences with a propensity to form guanine tetraplexes have been found in chromosomal telomers, immunoglobulin switch regions, and recombination sites. We report the crystal structure at 0.95 Å resolution of a parallel-stranded tetraplex formed by the hexanucleotide d(TG<sub>4</sub>T) in the presence of sodium ions. The four strands form a right-handed helix that is stabilized by hydrogen-bonding tetrads of co-planar guanine bases. Well-resolved sodium ions are found between and, at defined points, within tetrad planes and are coordinated with the guanine O6 groups. Nine calcium ions have been identified, each with a well-defined hepta-coordinate hydration shell. Hydrogen-bonding water patterns are observed within the tetraplex's helical grooves and clustered about the phosphate groups. Water molecules in the groove may form a hydrogen bond with the O4', and may affect the stacking behavior of guanine. Two distinct stacking arrangements are noted for the guanine tetrads. The thymine bases do not contribute to the four-stranded conformation, but instead stack to stabilize the crystal lattice. We present evidence that the sugar conformation is strained and propose that this originates from forces that optimize guanine base stacking. Discrete conformational disorder is observed at several places in the phosphodiester backbone, which results from a simple crankshaft rotation that requires no net change in the sugar conformation.

© 1997 Academic Press Limited

**Keywords:** guanine tetraplex; metal coordination; hydration structure; base stacking; X-ray crystallography

\*Corresponding author

## Introduction

For nearly 100 years, it has been known that polyguanylic acid can form polycrystalline gels in the presence of monovalent cations. Even the single nucleotide, guanine monophosphate, can form well-ordered gels. Gellert *et al.* (1962) proposed that the highly ordered structure arose from the assembly of guanine bases into square-planar groups that resemble macrocycles, in which the bases interact *via* hydrogen bonds. In this model, the N1 and N2 atoms of one base donate hydrogen bonds to the O6 and N7 atoms of an adjacent base, yielding eight hydrogen bonds per planar guanine ring (see Figure 1(a)). This model was subsequently

corroborated by fibre diffraction studies, which indicated that the planar rings readily stack in a helical fashion. Such stacking brings the O6 carbonyl oxygen atoms of adjacent tetrads into close proximity to form a binding site for small cations (Tougaard *et al.*, 1973; Arnott *et al.*, 1974; Zimmerman *et al.*, 1975; Zimmerman, 1976). Tetraplex structures formed by guanine oligonucleotides with either deoxyribose or ribose sugars have recently been characterised by X-ray diffraction and NMR studies (Aboul-ela *et al.*, 1992, 1994; Cheong & Moore, 1992; Kang *et al.*, 1992; Laughlan *et al.*, 1994; Schultze *et al.*, 1994; Smith & Feigon, 1993; Wang & Patel, 1992, 1993). These studies show that the strands can associate in parallel or a variety of antiparallel orientations, and thus generate a number of diverse conformations.

Until recently, it was not clear whether four-stranded DNA or RNA have any function in

Abbreviations used: d(TG<sub>4</sub>T), deoxyribose-(TpGpGpGpGpT); MPD, 2,4-methyl-pentane-diol.

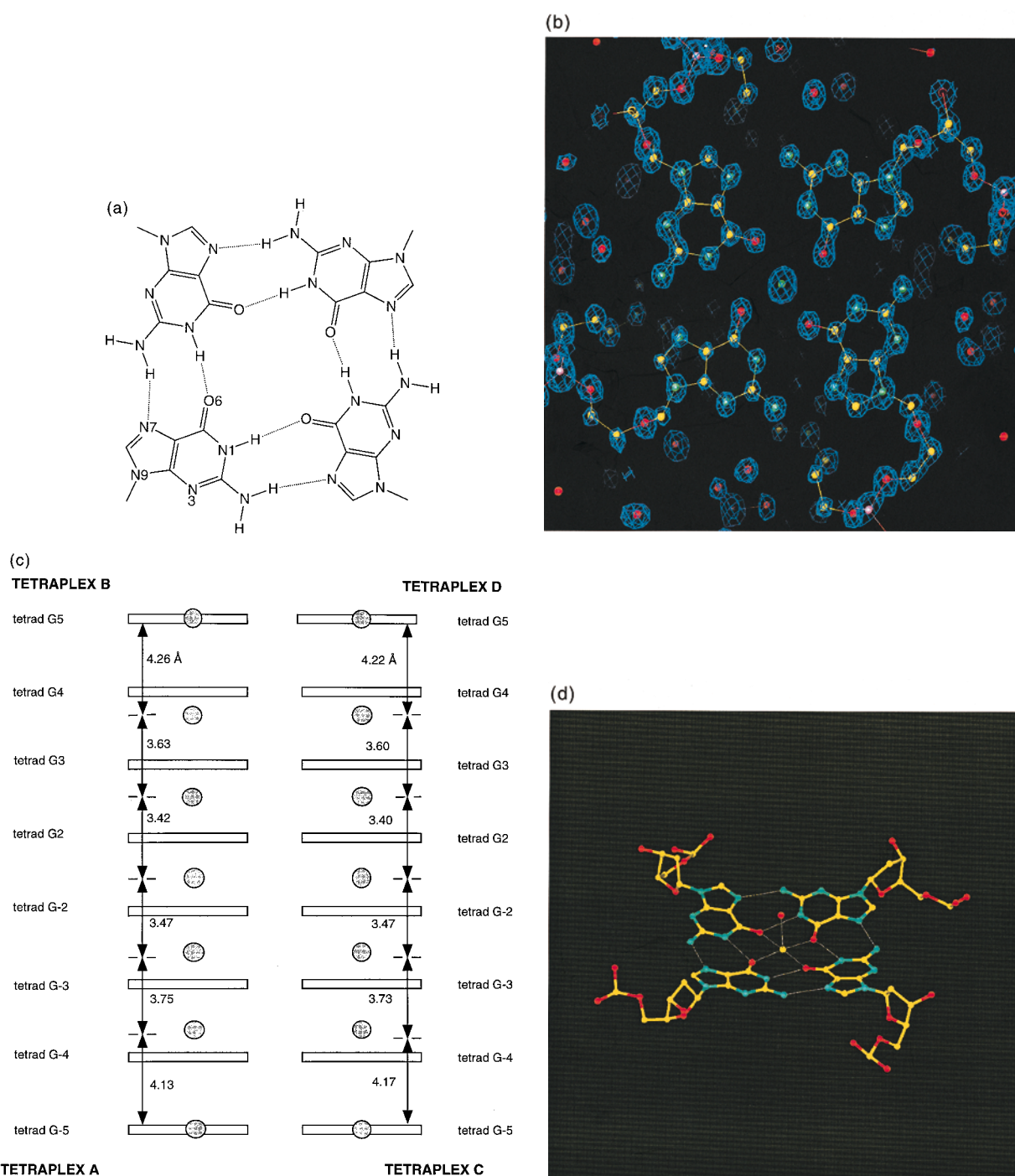


**Figure 1.** (a) Chemical structure of a tetrad. (b) Representative electron density showing sodium coordination at tetrad 1 of tetraplex A. The view is along the helical axis. The map was calculated using  $2F_o - F_c$  coefficients at 0.95 Å. (c) Separation of Na ions between successive guanine tetrads. View is perpendicular to the helical axis. (d) The sodium coordination of the 3' tetrads, showing the water at the axial position of a pyrimidal coordination scheme.

cells, but accumulating evidence has implicated tetraplexes in a number of potential biological roles. Guanine tracts have now been identified in chromosomal telomeres in organisms throughout the animal kingdom (Blackburn, 1991) and the immunoglobulin switch regions of higher organisms (Sen & Gilbert, 1988). These sequences have been shown to associate by hydrogen bonding *in vitro* to form four-stranded DNA (Sen &

Gilbert, 1988; Sundquist & Klug, 1989; Williamson *et al.*, 1989). The functional relevance of tetraplexes has been further supported by the identification of proteins which recognise and promote the formation of four stranded DNA structures *in vitro* (Fang & Cech, 1993; Liu & Gilbert, 1994; Liu *et al.*, 1995; Rhodes & Giraldo, 1995). Indeed, the slow rates of formation and extreme stability of tetraplexes suggests that their

formation equilibria *in vivo* might be controlled by chaperone-like molecules.

The structure which we report here is related to the telomeric repeat sequence found in *Tetrahymena*, the unit of which is TTGGGG. We had crystallized the short DNA sequence, TGGGGT and reported previously the structure at 1.2 Å from data collected at 277 K (Laughlan *et al.*, 1994). In agreement with NMR studies of the same sequence (Aboul-ela *et al.*, 1992, 1994), the DNA was found to form a parallel-stranded, right-handed helix. The crystal structure revealed sodium ions coordinated to the guanine bases in the central cavity of the helix. The diffraction data have now been extended to 0.95 Å using data collected at 100 K, and the high-resolution model has been refined. We describe the details of the tetraplex stereochemistry and hydration patterns in this higher resolution structure.

## Results and Discussion

Despite the simplicity of the constituent hexanucleotide, the asymmetric unit of the d(TGGGGT) crystals is complex, for it is comprised of four independent tetraplexes (Figure 2). The four molecules can be grouped into two pseudo-equivalent sets in which a pair of tetraplexes are co-axially stacked with a 5' to 5' orientation. This generates a ladder of eight stacked tetrads. In both sets, sodium ions lie at discrete points on the DNA axis. Calcium ions lie on the equator of the unit cell, and stabilise contacts between adjacent tetraplexes. The convention used in this paper to identify the tetrads is indicated in Figure 2(a).

In Figure 1(b), the electron density is shown for one of the central guanine tetrads at the interface between two stacked tetraplexes (i.e. tetrads of the type G-2/G2). The tetrad is planar and is stabilised by eight hydrogen bonds (Figure 1(a)). The electron density also clearly defines a sodium ion which lies outside the plane of this guanine tetrad. The sugar and phosphate backbone are also clearly defined throughout the structure, as indicated by the representative electron density shown in Figure 3(a) and (b).

The central core of the stacked tetraplexes has a line of seven sodium ions that are coincident with helical axes. The intermolecular ion between the stacked tetraplexes is equidistant from the upper and lower tetrad (i.e. tetrads of the type G2 and G-2). Here, the metal is bipyrimidally coordinated by eight equidistant carbonyl oxygen atoms. However, the sodium ions that are within a tetraplex deviate from the symmetrical geometry: the metals are slightly displaced in the 3' direction, and this displacement grows larger as one moves toward the 3' termini (Figure 1(c)). Indeed, the terminal sodium is so greatly displaced that it has become co-planar with the guanine bases (Figure 1(d)). A water molecule is coordinated axially to the terminal sodium ion, and forms a hydrogen bond

with a thymine from a tetraplex in the neighbouring asymmetric unit. The noted displacements of the ions within the tetraplexes may arise from electrostatic repulsion of the sodium ions in adjacent tetrads. In this regard, the stability of the tetraplex might seem a puzzle, since the sodium ions approach so closely. However, the sodium-sodium repulsion may be partially shielded throughout the structure by the partial electronegative charges of the coordinating carbonyl groups, which may be as great as half a charge (MacKerell *et al.*, 1995).

As one moves toward the 3' end of each tetraplex, the separation of carbonyl oxygen atoms within each tetrad increases and the tetrad planes buckle. These adjustments may be required to accommodate the asymmetrically displaced sodium ions.

The 1.2 Å structure reported earlier was studied at 277 K, while the 0.95 Å structure was studied at 100 K. The lower temperature compresses the cell by 1.0 to 1.9% along each axis (Table 1). The compression is principally along the helical axis of both stacked tetraplex pairs (i.e. pairs A/B and C/D in Figure 2), and the associated structural changes are small and distributed.

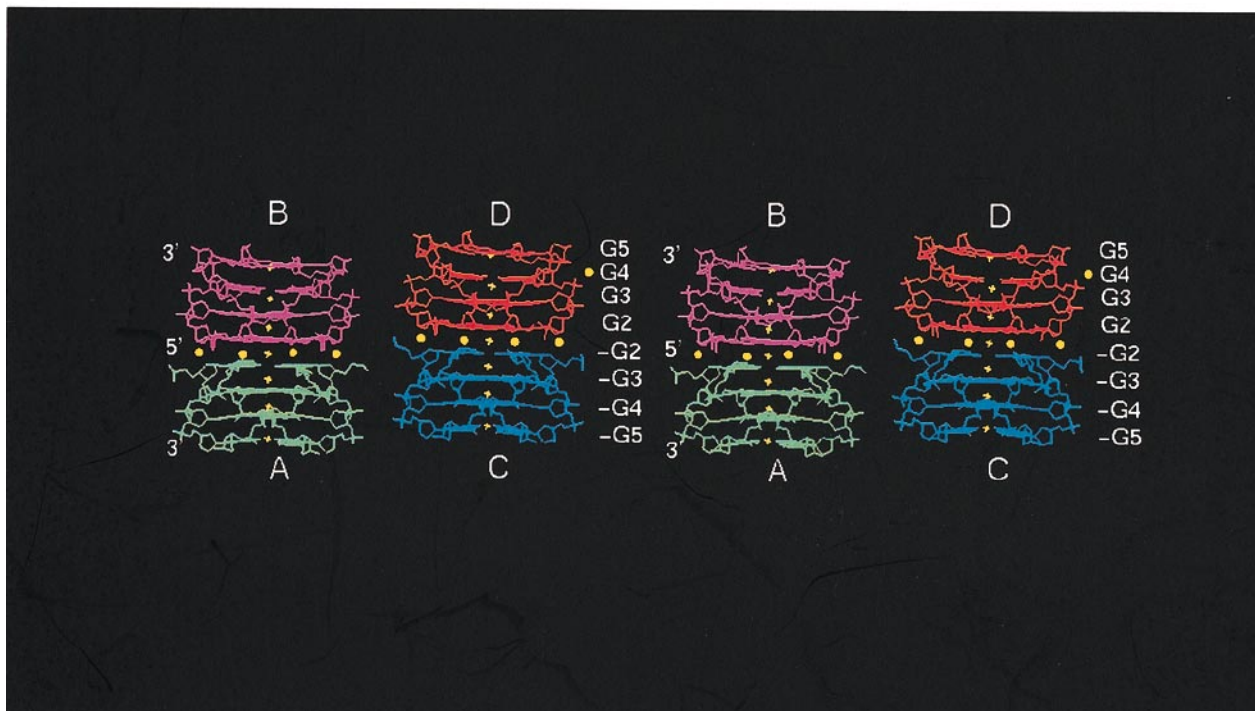
### Base-stacking interactions

The stacking of tetrads within and between tetraplexes differ, as shown in Figure 4. An example of tetrad stacking within a tetraplex is shown in Figure 4(b). Here, the six-membered ring of the 3' guanine base lies over the five-membered ring of the 5' guanine base, which is similar to the stacking arrangement seen in poly(dG)-poly(dC) duplex DNA (McCall *et al.*, 1984). A second type of stacking interaction occurs at the 5'-5' interface between coaxial tetraplex molecules, where five-membered rings are almost maximally overlapped (Figure 4(a)). In projection, this resembles a decagon, where the vertices of one five-membered ring lie between those of the ring below. The stacking geometry brings the carbonyl oxygen atoms of the upper and lower tetrads into proximity. It is interesting to note that a similar stacking contact is observed in antiparallel tetraplexes (Kang *et al.*, 1992; Wang & Patel, 1992, 1993).

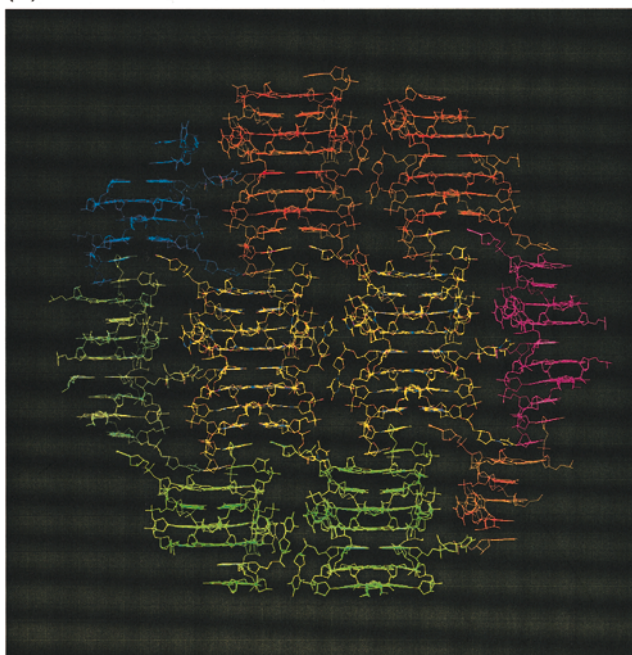
### Counterion interactions

The crystal lattice order was greatly improved by the addition of calcium ions, implying a stabilizing role for these ions. We have identified nine calcium counterions in the electron density map (Figure 5), all of which cross-bridge neighbouring tetraplexes. Eight of the calcium ions lie in two planes running through the 5'-5' interfaces which are normal to the helical axes (Figure 2(a)). The remaining ninth calcium ion can be viewed to the left of tetraplex A, midway down the length of the tetraplex (Figure 2(a)). This ion would appear to contribute to the non-equivalence of the two tetraplex pairs.

(a)



(b)



(c)

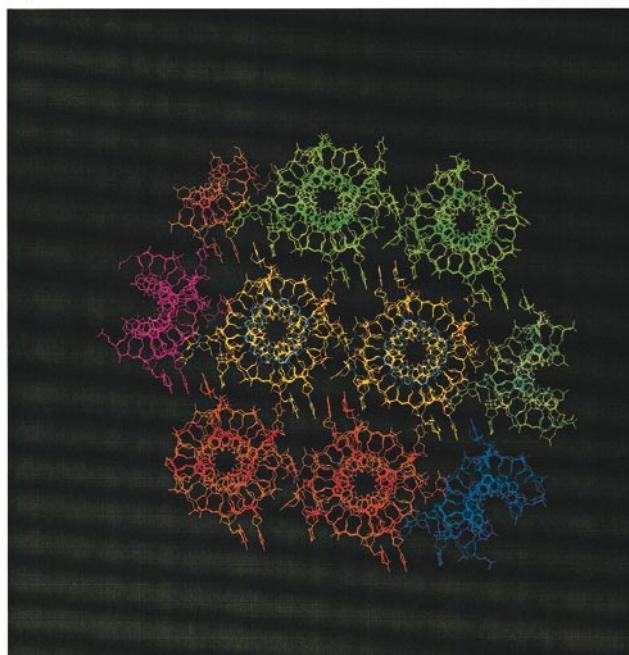


**Figure 2.** (a) Stereoscopic view of the contents of the asymmetric unit, with labelling scheme shown to identify the four tetraplexes (A,B,C and D), the four guanine tetrads within each tetraplex (2,3,4,5 for B and D; -2,-3,-4 and -5 for A and C) and the phosphate backbone. Sodium ions are indicated by yellow crosses and calcium ions by yellow spheres. For clarity, water molecules and thymine bases have been removed. (b) View of the cell perpendicular to the helical axes, showing that the axes of tetraplexes in neighbouring cells are parallel, but translated. Interdigitation of thymine groups can also be seen. (c) View of the unit cell contacts along the helical axes. The stacking of the thymine bases can be seen.

Nearly all the calcium ions coordinate seven water molecules (Figure 5), which in turn donate hydrogen bonds to phosphate oxygen atoms and stabilise a second hydration shell.

One calcium ion, making the exception to the rule, takes a thymine O4 as the seventh ligand. The  $\text{Ca}^{2+}$ -oxygen distances vary between 2.33 and 2.56 Å.

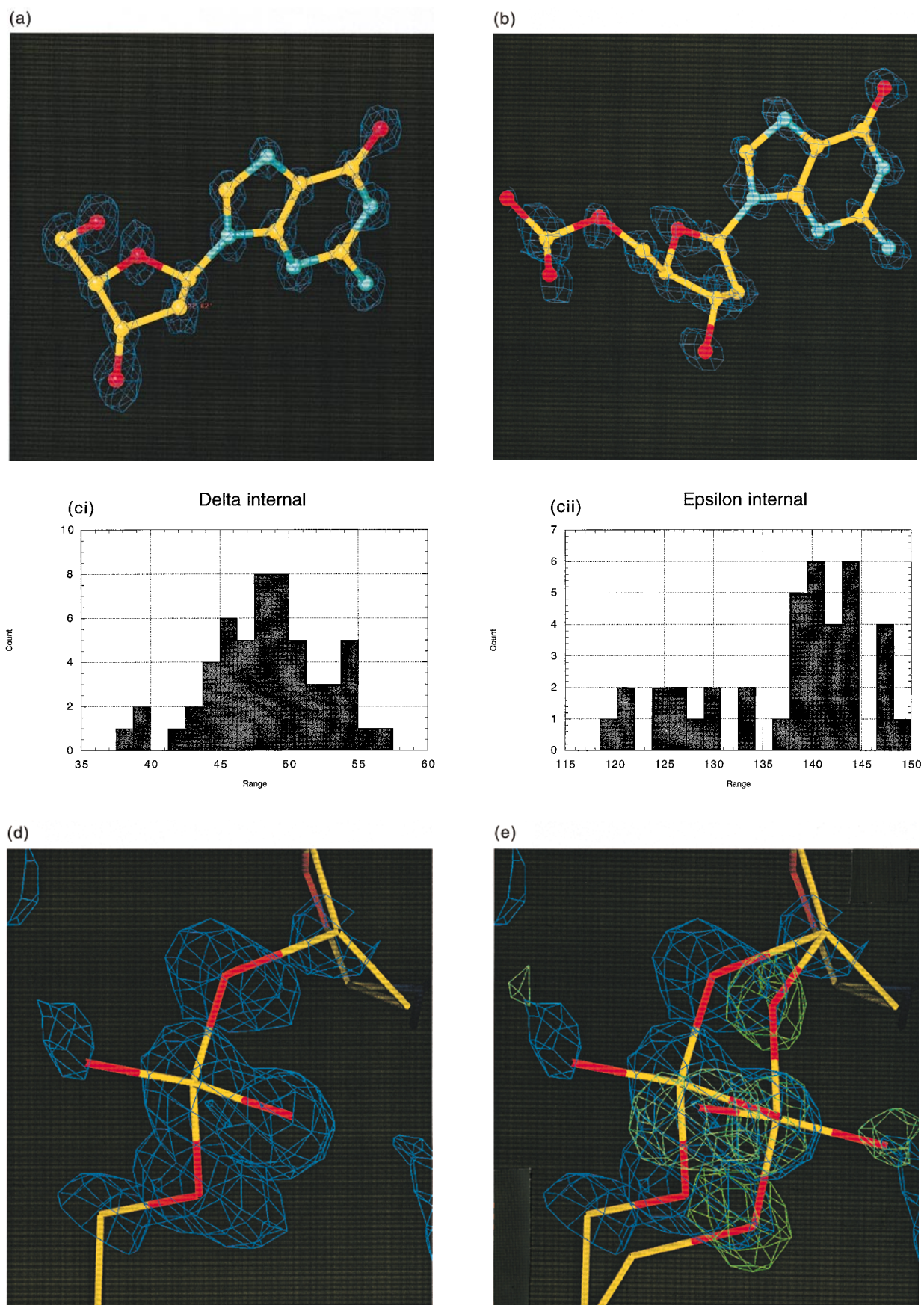


**Figure 3.** (a) The electron density for the two principal furanose conformations C2' *endo* (b) and C3' *endo*. (c) Torsion angle distributions for in the internal tetrads. The  $\delta$  and  $\epsilon$  values lie  $4\sigma$  and  $6\sigma$ , respectively, from the mean value for free nucleotides reported by Moodie & Thorton (1993). (d) A  $2F_o - F_c$  map showing the density at one of the phosphate groups and (e) a  $F_o - F_c$  difference map (green) and model for the phosphate backbone in two conformations.

**Table 1.** Cell dimensions and data quality

A. Cell dimensions						
Temperature (K)	<i>a</i>	<i>b</i>	<i>c</i> (Å)	$\alpha$	$\beta$	$\gamma$ (°)
270	28.76	35.47	56.77	74.39	77.64	89.73
100	28.28	34.78	56.23	74.31	77.68	89.81
B Data quality						
Resolution	<i>N</i> <sub>obs</sub> <sup>a</sup>	(% complete)		<i>R</i> -factor <sup>b</sup>	$\langle I \rangle / \sigma I$	
2.57	4850	76.4		7.0	26.2	
2.05	5126	80.9		10.4	16.5	
1.79	5492	86.2		6.4	16.7	
1.62	5651	88.9		5.8	12.7	
1.51	5798	91.9		5.4	13.0	
1.42	5988	94.0		5.3	13.8	
1.35	5916	93.4		5.2	14.5	
1.29	5875	92.9		5.2	14.4	
1.24	5889	92.4		5.4	14.1	
1.20	5817	91.7		5.3	14.0	
1.16	5799	91.1		5.5	14.1	
1.13	5708	90.5		5.9	13.1	
1.10	5744	89.7		6.2	12.6	
1.07	5621	89.3		6.9	11.9	
1.05	5658	89.2		7.5	10.8	
1.02	5627	88.7		8.7	9.6	
1.00	5651	88.3		9.7	8.4	
0.98	5602	87.5		10.8	7.6	
0.97	5437	86.9		13.2	6.2	
0.95	5470	85.9		14.6	5.5	
Net	112,719	88.8		6.9		

<sup>a</sup> *N*<sub>obs</sub> is the number of unique reflections, after merging the data. The average measurement redundancy is 1.9.

<sup>b</sup>  $R\text{-factor} = \frac{\sum_i \sum_j |I(h)_i - \langle I(h) \rangle|}{\sum_i \sum_j |I(h)_i|}$ .

## Hydration patterns

The hydration structure in the grooves and about the phosphate groups is clearly discernable in the electron density maps (Figures 5 and 6(a)). The averaged intra-strand separation of phosphates in the four tetraplexes is 6.6 Å, which is similar to that of *B*-form DNA. Water molecules cluster around individual phosphate groups, but we do not observe any water molecules bridging

adjacent phosphate groups, as occurs in *A* and *Z* forms (Saenger *et al.*, 1986).

Because all its strands are parallel, the tetraplex studied here should have 4-fold symmetry, and indeed the four tetraplex grooves are found to be almost equivalent with respect to hydration structure. The four grooves are relatively narrow, varying between 2.3 and 3.3 Å in width as measured by cross-strand phosphate separations. Hence, they are favourable binding sites for water molecules,

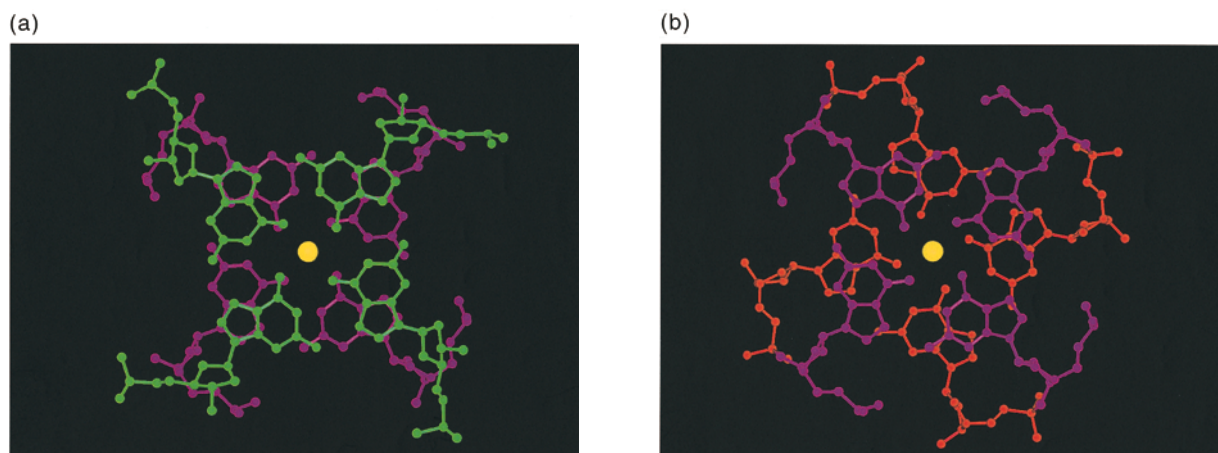


**Figure 4.** (a) Base-stacking interactions at the head-to-head interface between stacked tetraplexes (tetrads 2 in purple and -2 in green) and (b) within the tetraplex (tetrads 2 in purple and 3 in orange). The sodium ion is shown as the yellow circle.

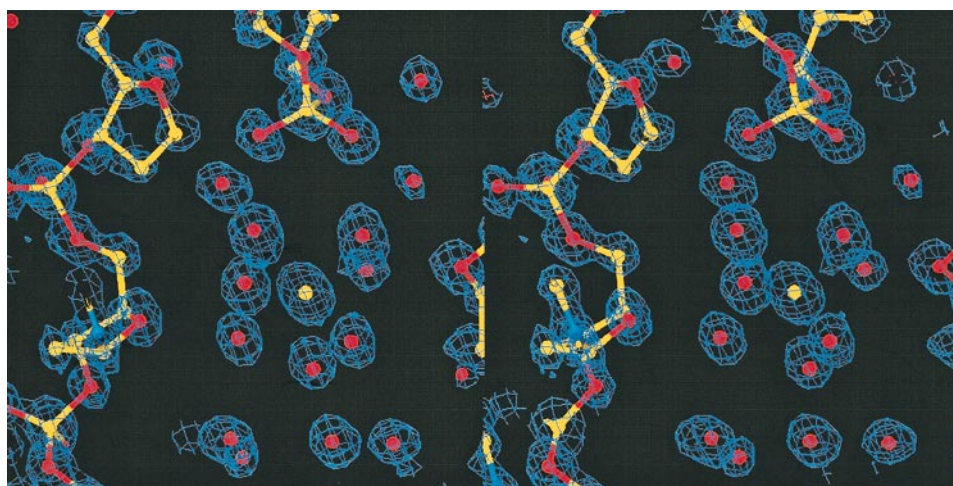


Figure 5. Stereoscopic view of the electron density revealing a representative calcium ion.

which form hydrogen bonds with the exposed N2 amino group, the heterocyclic N3 and with each other to create well supported networks (Figure 6(a) and (b)).

To examine patterns of hydration, we have superimposed the base atoms of 64 guanine-guanine pairs and plotted the distribution of water molecules (Figure 6(b)). One position seems to be

preferred where water molecules are localised by hydrogen bonding to the N2 and the N3 atoms. The other two favoured positions lie slightly out of the plane of the guanine base. These water molecules interact with either the N2 or N3 group of adjacent bases and the phosphate backbone or calcium counterions. The guanine hydration pattern in the tetraplex has some similarities to that of

(a)

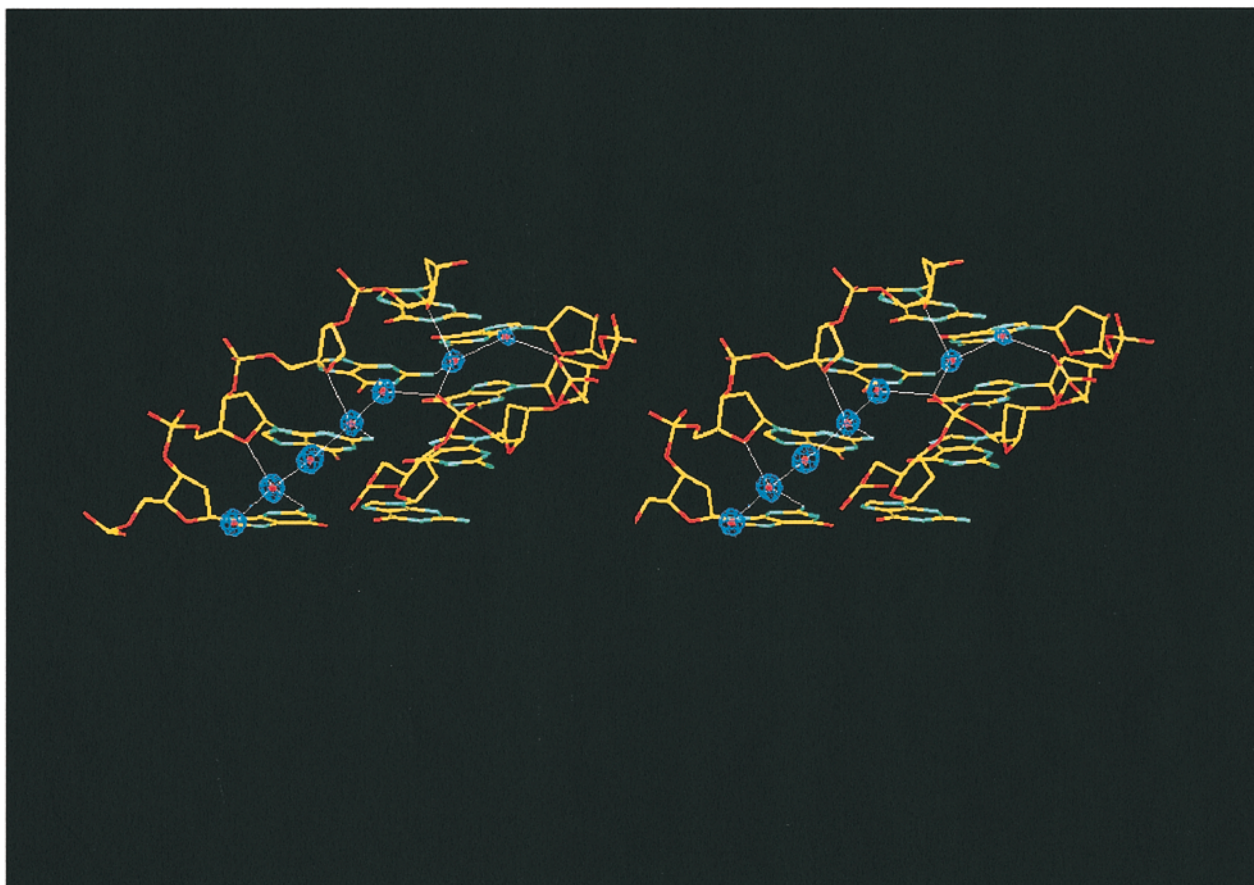
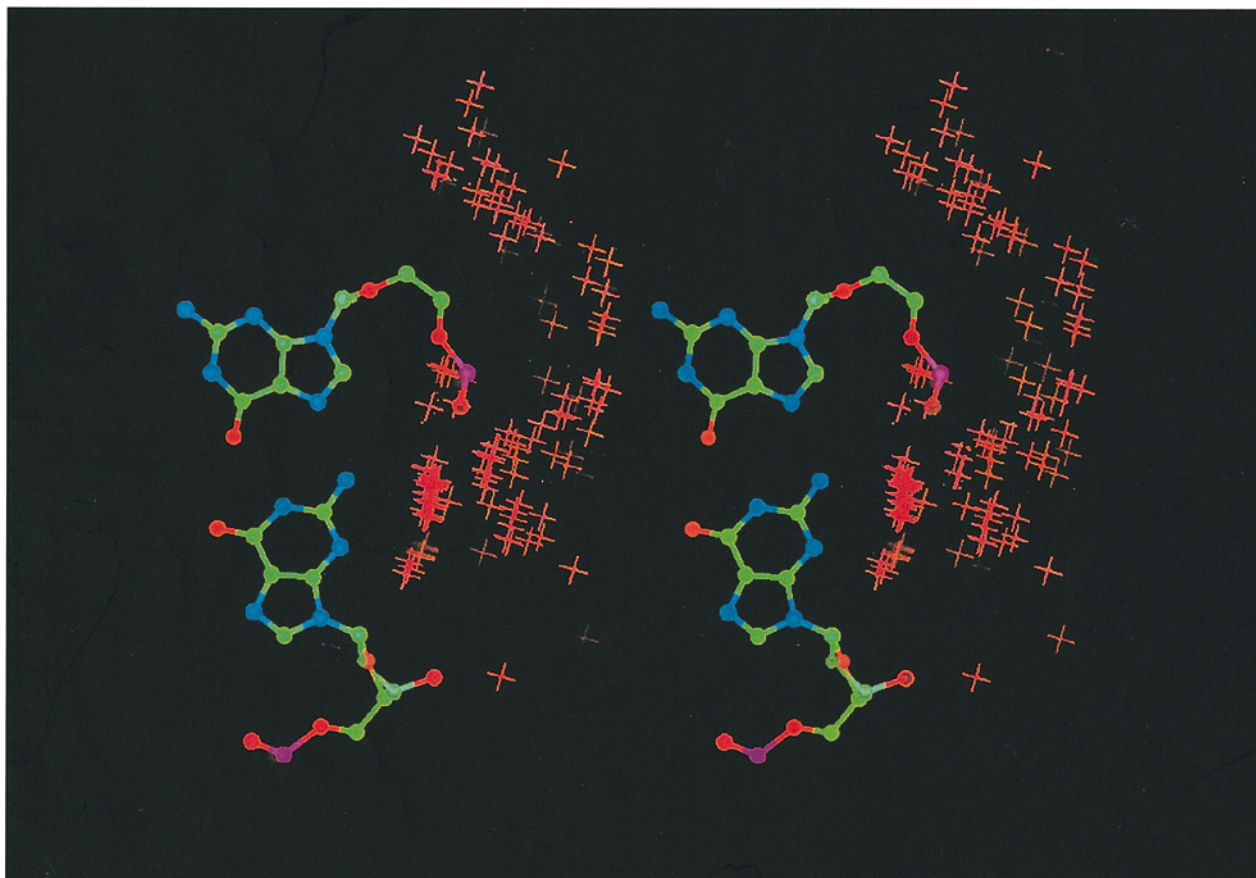
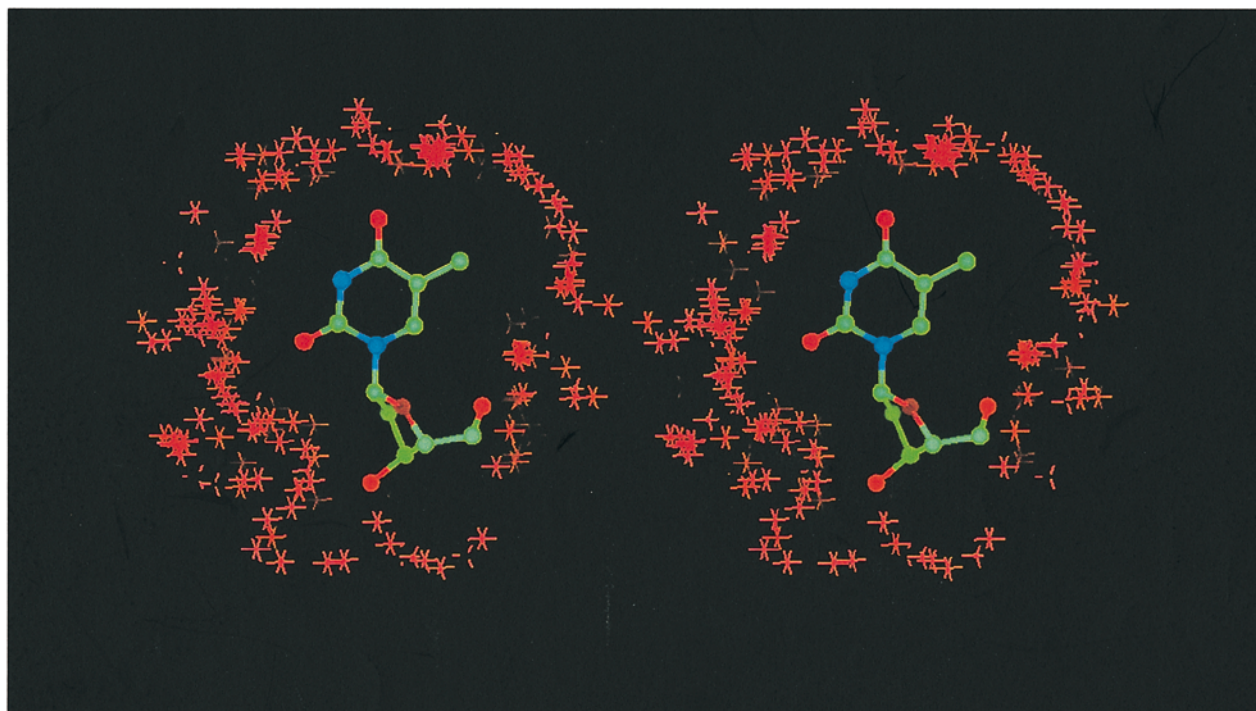


Figure 6(a) (legend on page 178)

(b)



(c)



**Figure 6.** (a) Stereoscopic view of the electron density of a representative groove, showing the hydration spine. All 16 crystallographically independent grooves have similar hydration spines. For clarity, the electron density is shown only for the water molecules (small red spheres). Hydrogen bonds are indicated by broken lines. (b) A stereoscopic view of hydration within the grooves: the distribution of water molecules around the averaged guanine:guanine base pair. (c) A stereoscopic view of the distribution of water molecules around the 28 observed thymine bases.

Z-DNA. In the latter, water molecules have a preference for N2 over N3 relative to the *B* and *A* forms, where N3 is preferred over the mostly unhydrated N2 (Schneider *et al.*, 1993).

We noted that water molecules are often found deep in the groove near each of the furanose oxygens (O4'; Figure 6(a)). These water molecules are linked together in a spine by a second layer of water molecules. The deeper molecules accept hydrogen bonds from the N2 atom (mean N2–water oxygen atom distance is 2.95(±0.05) Å) and interact with two of the second layer molecules. The mean water oxygen to O4' distance is 2.80(±0.05) Å, and many of the distances lie within van der Waals radii. The O4' lies at the apex of a tetrahedral pyramid about the water molecule (Figure 6(a)). Its close contact and geometry suggests that the water molecule donates a hydrogen bond to the furanose oxygen atom. As the water molecule links the guanine N2 with the sugar of the adjacent base, it might affect the preferred base-stacking geometry.

In Figure 6(c), we have superimposed the thymine base atoms for all 28 ordered thymine bases of the model, and have included water molecules within a 5 Å radius. This might be considered as a sampling of the ensemble of available water networks. It is apparent visually that water molecules cluster at the N3 position. There is also a weaker bimodal distribution about the O2 and O4, which is similar to the patterns observed by Schneider *et al.* (1993) for thymine in *B*-DNA. It seems likely that the preferred patterns of the primary hydration shell occur in the exposed base when free in solution and must be displaced during strand association, contributing a favourable entropic component to the free energy of this process.

The non-polar 5-methyl group is partially exposed to the solvent, which is thermodynamically unfavourable. Others have noted that water can form defined structures (pentagons, in particu-

lar) around exposed non-polar groups in protein structures (Teeter *et al.*, 1993; Bouquiere *et al.*, 1994). There is no analogous water ordering around the thymine methyl group, which is never entirely exposed to solvent since the stacking of the thymine bases partly occludes the methyl group (Figure 2(b) and (c)). Consequently, only a band across the surface of the methyl group is exposed to the solvent, and this may not be sufficient to drive water ordering.

### Stereochemistry of the sugar and phosphodiester backbone

Owing to the clear definition of the electron density maps, the pucker of all the sugar rings can be determined unambiguously. Almost all have pseudorotation angles that fall within the ranges described for ideal *B*-form DNA (Figure 3(b); Table 2). However, the four sugar rings in the G2 tetrads of tetraplexes B and D at the 5'-5' interface (but not the G-2 tetrad of tetraplexes A and C) assume a 3'-*exo* pucker, similar to that of *A*-form DNA (Figure 3(a)). This occurs in order to avoid steric clash between the O4' groups of G2 with those of the neighbouring tetrad G-2. For the subset of the eight G2 tetrad sugars of tetraplexes B and D, the average pseudorotation phase angle is 38.4(±9.3)°, while for the remaining 56 guanine nucleotides, the average is 150.3(±21.0)°. This switch in sugar conformation constitutes the only apparent anomaly in the conformational similarity of the four tetraplex structures in the unit cell.

Table 2 summarises the torsion angles of the phosphate backbone. The values of all torsion angles lie within a tight distribution, with the exception of the  $\delta$  and  $\epsilon$  angles found for the interface sugars of G2 tetrads. As noted above, these sugars also have profoundly different pseudorotation phase angles. The distribution of the values of the  $\delta$  and  $\epsilon$  angles in the 56 internal tetrads are

**Table 2.** Sugar and phosphate stereochemistry

A. Sugar torsion and pseudo-rotation angles							
Group	$\nu_0$	$\nu_1$	$\nu_2$	$\nu_3$	$\nu_4$	$P^a$	
Junction	−13.9 (14.9)	−11.5 (12.8)	31.0 (4.6)	−39.5 (3.8)	33.9 (4.8)	38.4 (9.3)	
Internal	−24.6 (11.1)	34.3 (5.5)	−29.9 (5.7)	15.5 (8.7)	6.3 (10.4)	150.3 (21)	
B. Sugar-phosphate backbone torsion angle summary <sup>b</sup>							
Group	$\alpha$	$\beta$	$\gamma$	$\delta$	$\epsilon$	$\zeta$	$\chi$
Junction	–	–	151.4 (32.8)	183.1 (8.2)	86.5 (4.5)	198.4 (4.5)	181.4 (1.9)
Internal	265.4 (14.5)	288.6 (16.2)	190.3 (18.9)	48.6 (4.1)	136.8 (8.2)	182.9 (12.4)	245 (6.7)

Values represent means over the group and, in parentheses, the standard deviation. There are eight samples in the junctions group (tetrads B2 and D2) and 56 in the internal group (representing tetrads A2,A3,A4,A5, B3,B4,B5, C2,C3,C4,C5, D3,D4 and D5). The angles were calculated using NEWHELIX93 (R. E. Dickerson).

<sup>a</sup>  $P = \arctan \{(\nu_4 + \nu_1) - (\nu_3 + \nu_0) / [2 \nu_2 (\sin 36^\circ + \sin 72^\circ)]\}$

<sup>b</sup> Mean and standard deviations for the tetrads where the angles are defined. The angles were calculated using NEWHELIX93 (R. E. Dickerson).

shown in Figure 3(c). These values lie outside of the reported range for free nucleotides and ideal *A* and *B* form DNA (Moodie & Thornton, 1993; Neidle, 1994), suggesting that the backbone of the parallel tetraplex may actually be strained in the crystal structure.

The helical trajectory of the parallel tetraplex molecule is relatively underwound, with 12 bases per turn, in comparison with both *B*-form DNA (10.5 bases/turn) and *A*-form (11 bases/turn). This distinctive twist may optimise guanine stacking. The energetic penalty associated with any deviation from the optimal stacking will be quadrupled by virtue of the molecule's 4-fold symmetry. Therefore, there is a strong force to set the twist to an optimal value to maximise the attractive base-stacking interaction. As discussed above, the sugar conformations of the tetraplex resemble those found in *B*-DNA, and this might appear to be inconsistent with an underwound helical structure. The strain in the phosphate backbone torsion angles of the tetraplex is probably an unavoidable consequence of forcing the twist to optimize guanine stacking. In duplex DNA, local adjustments may occur to compensate for alteration in helical repeat, such as rolling and sliding motions; however, these movements may not be available for the tetraplex so that the backbone might become strained as a consequence.

The  $\chi$  angle, which describes the rotational positioning of the base with respect to the sugar, typically extends between  $180^\circ$  and  $300^\circ$  for the *anti*-conformation of purine nucleosides (Saenger, 1984). As shown in Table 2, the guanine bases in the parallel tetraplex are exclusively in the *anti*-conformation. NMR studies also show that the bases are *anti* in solution (Aboul-ela *et al.*, 1994). This is in contrast to the regular alternation between *syn* and *anti*-glycosyl torsion angles found in consecutive guanine bases in antiparallel tetraplexes (Kang *et al.*, 1992; Wang & Patel, 1992, 1993; Smith & Feigon, 1993; Wang *et al.*, 1991). While the  $\chi$  values for the G2 sugar residues at the head-to-head junction (which have the unusual pseudorotation phase angles) have values near  $180^\circ$ , the range for the internal tetrads lie roughly between  $240$  and  $250^\circ$ .

The high resolution of the data also permitted the unambiguous identification of discrete disorder in the phosphate backbone. The initial  $2F_o - F_c$  map revealed depleted density at certain O1P groups, but inflated density for the O2P, with elliptical density for the O5' and O3' groups (Figure 3(d)). Studying a  $F_o - F_c$  difference map, it became clear that this arises because the phosphate backbone assumes an alternative conformation, which places the phosphorus atom close to the original O2P position (Figure 3(e)). Five points of such disorder were found. It is interesting to note that the disorder is not propagated to the sugars on either side of the phosphodiester groups, as the density on the deoxyribose appears to be well-defined. This suggests that the switch in phosphate

backbone torsion angle does not require any net structural change in the sugar. Rotations in the sugar are most likely coupled tightly with the movements in the backbone that bring about the two discrete conformations. These observations suggest that, while the backbone in duplex DNA is quite flexible, it may have an highly anisotropic character. It might therefore be more appropriate to model the phosphate groups of crystal structures with anisotropic thermal disorder factors, rather than isotropic ones.

## Materials and Methods

### Oligonucleotide synthesis and purification

Oligonucleotides were synthesized using  $\beta$ -cyanoethyl phosphoramidite chemistry (Beaucage & Caruthers, 1981; Sinha *et al.*, 1984) implemented on a 394 DNA/RNA synthesiser (Applied Biosystems) without 5' deprotection. They were purified by reverse-phase chromatography (NENSORB, Dupont), followed by detritylation.

### Crystallization and data collection

The purified d(TG<sub>4</sub>T) was dissolved at 6 to 12 mM concentration in 5 mM Hepes (pH 7.0) and 0.1 M NaCl, and tetraplex formation was induced by slow cooling from  $70^\circ\text{C}$ . The annealed sample was then dialysed against 50 mM NaCl and concentrated using a 3 kDa molecular mass cutoff membrane (Centricon-3, Amicon, Beverly, MA).

The crystals were grown from high concentrations of NaCl and require CaCl<sub>2</sub> for improved order. Crystals were grown at 4 to  $6^\circ\text{C}$  by vapour diffusion from hanging droplets containing 20 mM sodium cacodylate-HCl (pH 6.6), 12 mM CaCl<sub>2</sub>, 6 mM spermine tetrahydrochloride, 130 to 180 mM NaCl, 5% (v/v) 2,4-methylpentanediol (MPD) and 1 mM d(TG<sub>4</sub>T). The droplets were equilibrated against reservoirs containing 120 mM sodium cacodylate-HCl (pH 6.6), 70 mM CaCl<sub>2</sub>, 700 mM to 1 M NaCl, and 26 to 32% MPD. Crystals grew within two weeks to a typical size of  $300\ \mu\text{m} \times 200\ \mu\text{m} \times 200\ \mu\text{m}$ . The crystals were often twinned and in some cases required manual dissection.

In preparation for cryogenic data collection, crystals were isolated in a small fibrous loop, immersed in neat mother liquor and then rapidly exposed to a dry nitrogen stream at 100 K. Data were measured from one crystal at Station BW7B at DESY, Hamburg using  $0.93\ \text{\AA}$  wavelength radiation. The diffraction pattern below  $2\ \text{\AA}$  resolution was problematic due to crystal twinning, and this diminished the quality of the data; however, the higher resolution data were free of twinning patterns and are of good quality. To correct for the poorer low resolution data, additional diffraction measurements were collected at Station 9.5 at SRS, Daresbury Laboratory from 20 to  $2\ \text{\AA}$  resolution. Data were processed and integrated using DENZO (Otwinowski, 1993). A total of 112,719 reflections are in the unique data set, representing 88.8% of all the reflections to  $0.95\ \text{\AA}$ . The cell dimensions and the quality of the merged data set is summarised in Table 1.

## Structure refinement

The starting model was the 1.2 Å structure refined earlier from data collected at 4°C (Laughlan *et al.*, 1994). The water structure was initially rebuilt using an automated water refinement procedure (ARP; Lamzin & Wilson, 1993) and SHELXL93 (Sheldrick, 1993). The refinement was constrained for atom-pair distances only, using parameters derived from a recent DNA database (Parkinson *et al.*, 1996) and block-diagonal matrices. The refined model includes 590 water molecules and contributions of hydrogen atoms, anisotropic temperature factors for all non-hydrogen atoms, and bulk-solvent. The free *R* factor was monitored throughout the early stages of refinement to test each step of the procedure. The final *R*-factor is 15.2% for all data and the goodness-of-fit  $[\sum_h \{F_{\text{obs}}(h)^2 - F_{\text{calc}}(h)^2\} / (n-p)]^{0.5}$  is 1.75, where *n* is the number of reflections and *p* is the total number of refined parameters. The r.m.s. bond length deviation from ideality is 0.016 Å. The final *R*-factor is higher than expected, and this may be due to the poorer quality of the low resolution data and to disorder of five thymine bases, which could not be observed even at the last stage of refinement and map interpretation.

## Acknowledgments

We thank Dr Nicola Arbuckle for help with data collection and the staff of DESY Hamburg and SRS Daresbury for use of facilities. We acknowledge support of an EU LISP award for access to large facilities. This study was supported by the Cancer Research Campaign (A. I. H. M and D. M. J. L), the Medical Research Council (K. P.) and the Wellcome Trust (K. P. and B. L.). We also wish to acknowledge helpful suggestions of the referees. The coordinates and data have been deposited with the Nucleic Acid Structure Databank and are available from the authors until they have been processed and released. This work is dedicated to Giulio Fermi.

## References

- Aboul-ela, F., Murchie, A. I. H. & Lilley, D. M. J. (1992). NMR study of parallel-stranded tetraplex formation by the hexadeoxynucleotide d(TG<sub>4</sub>T). *Nature*, **360**, 280–282.
- Aboul-ela, F., Murchie, A. I. H., Norman, D. G. & Lilley, D. M. J. (1994). Solution structure of a parallel-stranded tetraplex formed by d(TG<sub>4</sub>T) in the presence of sodium ions by nuclear magnetic resonance spectroscopy. *J. Mol. Biol.* **243**, 458–471.
- Arnott, S., Chandrasekaran, R. & Marttila, C. M. (1974). Structures for polyinosinic acid and polyguanylic acid. *Biochem. J.* **141**, 537–543.
- Beaucage, S. L. & Caruthers, M. H. (1981). Deoxynucleoside phosphoramidites – a new class of key intermediates for deoxypolynucleotide synthesis. *Tetrahedron Letters*, **22**, 1859–1862.
- Berman, H. M. (1991). Hydration of DNA. *Curr. Opin. Struct. Biol.* **1**, 423–427.
- Berman, H. M. (1994). Hydration of DNA: take 2. *Curr. Opin. Struct. Biol.* **4**, 345–350.
- Blackburn, E. H. (1991). Structure and function of telomeres. *Nature*, **350**, 569–573.
- Bouquiere, J. P., Finney, J. L. & Savage, H. F. J. (1994). High-resolution neutron study of vitamin B12 coenzyme at 15 K: solvent structure. *Acta Crystallog. sect. B*, **50**, 566–578.
- Cheong, C. & Moore, P. B. (1992). Solution structure of an unusually stable RNA tetraplex containing G and U-quartet structures. *Biochemistry*, **31**, 8406–8414.
- Fang, G. & Cech, T. R. (1993). The β subunit of *Oxytricha* telomere-binding protein promotes G-quartet formation by telomeric DNA. *Cell*, **74**, 875–885.
- Gellert, M., Lipsett, M. N. & Davies, D. R. (1962). Helix formation by guanylic acid. *Proc. Natl Acad. Sci. USA*, **48**, 21013–2018.
- Kang, C., Zhang, X., Ratliff, R., Moyzis, R. & Rich, A. (1992). Crystal structure of four-stranded *Oxytricha* telomeric DNA. *Nature*, **356**, 126–131.
- Lamzin, V. S. & Wilson, K. S. (1993). Automated refinement of protein models. *Acta Crystallog. sect. D*, **49**, 129–147.
- Laughlan, G., Murchie, A. I. H., Norman, D. G., Moore, M. H., Moody, P. C. E., Lilley, D. M. J. & Luisi, B. (1994). The high-resolution crystal structure of a parallel-stranded guanine tetraplex. *Science*, **265**, 520–524.
- Liu, Z. & Gilbert, W. (1994). The yeast KEM1 gene encodes a nuclease specific for G4 tetraplex DNA: implications of *in vivo* functions for this novel DNA structure. *Cell*, **77**, 1083–1092.
- Liu, Z., Lee, A. & Gilbert, W. (1995). Gene disruption of a G4-DNA-dependent nuclease in yeast leads to cellular senescence and telomere shortening. *Proc. Natl Acad. Sci. USA*, **92**, 6002–6006.
- MacKerell, A. D., Wiorkiewicz-Kuczera, J. & Karplus, M. (1995). An all-atom empirical energy function for the simulation of nucleic acids. *J. Am. Chem. Soc.* **117**, 11946–11975.
- McCall, M., Brown, T. & Kennard, O. (1985). The crystal structure of d(G-G-G-G-C-C-C). A model for poly(dG)-poly(dC). *J. Mol. Biol.* **183**, 385–396.
- Moodie, S. L. & Thornton, J. M. (1993). A study into the effects of protein binding on nucleotide conformation. *Nucl. Acids Res.* **21**, 1369–1380.
- Neidle, S. (1994). *DNA Structure and Recognition*. IRL Press, Oxford.
- Otwinowski, Z. (1993). Oscillation data reduction program. *Proceedings of the CCP4 Study Weekend* (Sawyer, L., Isaacs, N. & Bailey, S., eds), pp. 56–62, SERC Daresbury, UK.
- Parkinson, G., Vojtechovsky, J., Clowney, L., Brünger, A. T. & Berman, H. M. (1996). New parameters for the refinement of nucleic acid containing structures. *Acta Crystallog. sect. D*, **52**, 57–64.
- Rhodes, D. & Giraldo, R. (1995). Telomere structure and function. *Curr. Opin. Struct. Biol.* **5**, 311–322.
- Saenger, W. (1984). *Principles of Nucleic Acid Structure*. Springer-Verlag Inc., New York.
- Saenger, W., Hunter, W. N. & Kennard, O. (1986). DNA conformation is determined by economics in the hydration of phosphate groups. *Nature*, **324**, 385–388.
- Schneider, B., Cohen, D. M., Schleifer, L., Srinivasan, A. R., Olson, W. K. & Berman, H. M. (1993). A systematic method for studying the spatial distributions of water-molecules around nucleic acid bases. *Biophys. J.* **65**, 2291–2303.
- Schultze, P., Smith, F. W. & Feigon, J. (1994). Refined solution structure of the dimeric quadruplex formed from the *Oxytricha* telomeric oligonucleotide d(GGGGTTTGGGG). *Structure*, **2**, 221–233.

- Sen, D. & Gilbert, W. (1988). Formation of parallel-stranded complexes by guanine-rich motifs in DNA and its implications for meiosis. *Nature*, **334**, 364–366.
- Sheldrick, G. M. (1993). SHELXL-93, Göttingen.
- Sinha, N. D., Biernat, J., McManus, J. & Koster, H. (1984). Polymer support oligonucleotides synthesis XVIII: Use of  $\beta$ -cyanoethyl-*N*-*N*-dialkylamino/*N*-morpholino phosphoramidite of deoxynucleosides for the synthesis of DNA fragments simplifying deprotection and isolation of the final product. *Nucl. Acids Res.* **12**, 4539–4557.
- Smith, F. W. & Feigon, J. (1993). Strand orientation in the DNA quadruplex formed from the *Oxytricha* telomere repeat oligonucleotide d(G<sub>4</sub>T<sub>4</sub>G<sub>4</sub>) in solution. *Biochemistry*, **32**, 8682–8692.
- Sundquist, W. I. & Klug, A. (1989). Telomeric DNA dimerizes by formation of guanine tetrads between hairpin loops. *Nature*, **342**, 825–829.
- Teeter, M. M., Roe, S. M. & Heo, N. H. (1993). Atomic resolution (0.83 Å) crystal structure of the hydrophobic protein crambin at 130 K. *J. Mol. Biol.* **230**, 292–311.
- Tougaard, P., Chantot, J.-F. & Guschlbauer, W. (1973). Nucleoside conformations X. An X-ray fibre diffraction study of the gels of guanine dinucleosides. *Biochim. Biophys. Acta*, **308**, 9–16.
- Wang, Y. & Patel, D. J. (1992). Guanine residues in d(T<sub>2</sub>AG<sub>3</sub>) and d(T<sub>2</sub>G<sub>4</sub>) form parallel-stranded potassium cation stabilized G-quadruplexes with *anti* glycosidic torsion angles in solution. *Biochemistry*, **31**, 8112–8119.
- Wang, Y. & Patel, D. J. (1993). Solution structure of a parallel-stranded G-quadruplex DNA. *J. Mol. Biol.* **234**, 1171–1183.
- Wang, Y., de los Santos, C., Gao, X., Greene, K., Live, D. & Patel, D. J. (1991). Multinuclear nuclear magnetic resonance studies of Na cation-stabilised complex formed by d(G-G-T-T-T-T-C-G-G) in solution. *J. Mol. Biol.* **222**, 819–832.
- Wang, K. Y., Kumar, S., Pham, T. Q., Marathias, V. M., Swaminathan, S. & Bolton, P. H. (1996). Determination of the number and location of the manganese binding sites of DNA quadruplexes in solution by EPR and NMR in the presence and absence of thrombin. *J. Mol. Biol.* **260**, 378–394.
- Williamson, J. R., Raghuraman, M. K. & Cech, T. R. (1989). Monovalent cation-induced structure of telomeric DNA: the G-quartet model. *Cell*, **59**, 871–880.
- Zimmerman, S. B. (1976). X-ray study by fiber diffraction methods of a self-aggregate of guanosine-5'-phosphate with the same helical parameters as poly(rG). *J. Mol. Biol.* **106**, 663–672.
- Zimmerman, S. B., Cohen, G. H. & Davies, D. R. (1975). X-ray fibre diffraction and model building studies of polyguanylic acid and polyinosinic acid. *J. Mol. Biol.* **92**, 181–192.

Edited by R. Huber

(Received 6 May 1997; received in revised form 21 July 1997; accepted 22 July 1997)